

# Models of Dark Matter and the INTEGRAL 511 keV line

Yonatan Kahn

Senior Honors Thesis

Advisor: Professor Tim Tait

May 5, 2009

Prepared in partial fulfillment of the requirements for the Physics Honors Degree,  
Northwestern University

## ABSTRACT

Two models of dark matter are examined in the context of the bright 511 keV gamma-ray signal observed from the center of the galaxy by the INTEGRAL satellite. A model of annihilating MeV-scale dark matter has been shown by Boehm *et al.* to be able to provide the required flux of positrons to explain the INTEGRAL signal, and the possible experimental consequences of this model are investigated in rare pion decays. A second possible explanation for INTEGRAL is considered, where TeV-scale WIMPS interacting with a GeV-scale scalar mediator produce positrons through formation and excitation of WIMP-WIMP bound states at the center of the galaxy. It is found that the MeV dark matter model could explain an observed excess in the decay  $\pi^0 \rightarrow e^+e^-$ , but that the TeV WIMP model is unable to explain INTEGRAL in the weak-coupling scenario. Brief concluding remarks are made about possible extensions of the TeV WIMP model to strongly coupled systems.

# 1 Introduction

The nature of dark matter has emerged as one of the most pressing questions facing physics today. Extensive astrophysical observations, including measurements of rotation curves of galaxies [1] and gravitational lensing of colliding clusters [2], have provided compelling empirical evidence for the existence of dark matter. Moreover, cosmological measurements of the matter and baryon density of the universe show that baryonic matter (i.e. protons and neutrons) comprises only 20% of the matter content of the universe, implying that non-baryonic dark matter must make up the rest [3]. Although dark matter is so named because it has no electromagnetic interactions and does not emit light, its existence is closely intertwined with the fate of baryonic matter in the universe, since dark matter “clumping” as the universe cooled may have been responsible for the formation of large-scale structure, such as galaxies [4].

Despite the wealth of observational evidence from astrophysics and cosmology, dark matter still has no place within the framework of particle physics. Neutrinos have been ruled out as a source of dark matter [5], and so the Standard Model contains no dark matter candidate; any particle candidate for dark matter will necessarily require an extension of the Standard Model with new particles and interactions. A popular candidate is the neutralino, found in supersymmetric extensions of the Standard Model as a combination of the superpartners of the neutral gauge bosons and Higgses. While the neutralino is attractive because its annihilation cross-section in the hot early universe is naturally of the same order of magnitude required to fix the correct relic density of dark matter [5], there has been no unambiguous direct detection of dark matter, and the door is still open for other, less conventional models.

The astrophysical and particle-physics consequences of two models of dark matter are considered in this thesis; a light scalar particle (1-3 MeV) interacting with a 10-100 MeV gauge boson, and TeV-scale scalar Weakly Interacting Massive Particle (WIMP) interacting with a GeV-scale scalar mediator. The stringent requirements placed on these models by constraints ranging from production of particles in the early universe to present-day collider experiments lead to interesting, but distinct, phenomenological signatures in both cases. In particular, it will be shown how the MeV dark matter model could lead to an enhancement of the rare decay  $\pi^0 \rightarrow e^+e^-$ . The common element to both models is their potential to explain the 511 keV gamma-ray signal from the center of the galaxy, which is discussed below.

## 2 The INTEGRAL 511 keV signal

The existence of a bright gamma-ray line emanating from the center of the galaxy has been known for decades. In 1972, Johnson *et al.* [6] used a balloon-hoisted NaI scintillation telescope to detect a 511 keV line from the galactic center. The energy of this line is significant because 511 keV is the mass of an electron, and such radiation is naturally explained by electron-positron annihilation. However, terrestrial positrons, such as those produced when cosmic rays hit the upper atmosphere, could be responsible for the radiation, without invoking annihilations at the center of the galaxy. After accounting for atmospheric effects,

though, Johnson *et al.* concluded that this line was significantly stronger than the cosmic background radiation from other directions at similar energies. Leventhal *et al.* [7] revisited this phenomenon in 1978 and identified the source of the radiation as positronium decay. Specifically, they concluded that positrons in the galactic center form both para-positronium, which annihilates to two photons, each at 511 keV, and ortho-positronium, which decays to three photons and contributes a spectrum of excess low-energy radiation at and below 511 keV. They also identified the majority of galactic positronium as para-positronium. Further experiments over the past 30 years [8, 9], and most recently the INTEGRAL satellite [10, 11], have refined the value of the observed photon flux and identified the majority of the radiation as coming from the galactic bulge. The spatial distribution of the line, long believed to be nearly spherical, has recently been measured by INTEGRAL to have a small longitudinal asymmetry [12].

Currently, the explanation of annihilating positronium is well-accepted as the source of the radiation, but the source of the positrons themselves remains unclear. Since our galaxy contains negligible amounts of antimatter, the measured flux of  $3 \times 10^{42} e^+$ /sec invites an explanation for such huge amounts of antimatter production. Several possibilities involving relatively well-known astrophysical phenomena have been put forth, including radioactive nuclei from supernovae [13], gamma-ray bursts [14], pulsars [15], black holes [16], and cosmic rays [17]. Most recently, the INTEGRAL collaboration [12] has identified several low-mass X-ray binaries (LMXBs), binary systems where one component is a compact object such as a neutron star or black hole, whose asymmetric distribution about the galactic center qualitatively matches the asymmetry of the 511 keV line. However, all these models have difficulty accounting for the high intensity of the photon flux except under rather restrictive assumptions. In particular, there exists no compelling model for the accretion of material into the LMXBs and the subsequent jet of high-energy photons which is supposed to produce the positrons, and the 511 keV flux could easily be underpredicted by an  $O(1) - O(10)$  factor.

If astrophysical explanations fail to explain the INTEGRAL measurements, then dark matter provides a natural solution. Except for the recently measured longitudinal asymmetry, the shape of the line qualitatively resembles the spherically-symmetric halo of dark matter which is expected to surround the galactic center. The constraints set by the INTEGRAL data on the dark matter mass and interactions can be used to search for the particles in direct detection experiments, providing an exciting link between astrophysical observations and terrestrial particle physics experiments. In the two dark matter models considered in this thesis, the INTEGRAL line results from annihilations of the MeV dark matter particles, or energy released in the formation of WIMP-WIMP bound states. These two possibilities, as well as their consequences for other aspects of the dark matter models, will be considered in the following two sections.

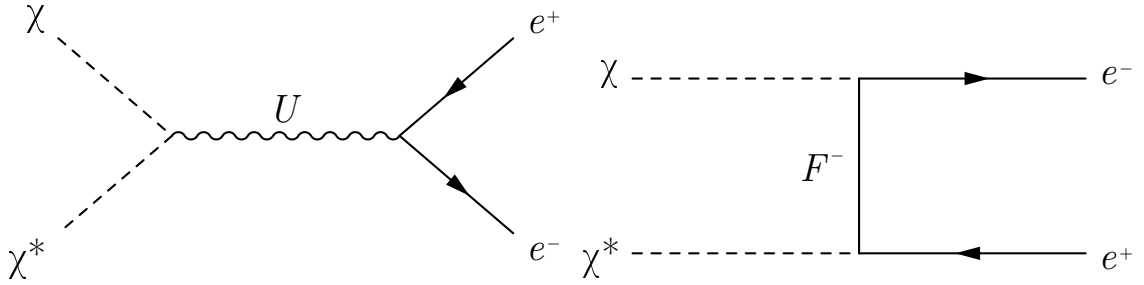


Figure 1: *Dark matter annihilation into an  $e^+e^-$  pair, through  $U$  boson exchange in the  $s$ -channel, and  $F^\pm$  fermion exchange in the  $t$ -channel*

### 3 Light dark matter

#### 3.1 Model description

Most models of dark matter have focused on the TeV mass scale not only because of supersymmetry, but because of the Lee-Weinberg limit [18], which sets a general lower bound of a few GeV on possible dark matter masses. In short, if the dark matter annihilation cross-section is proportional to  $m_{DM}^2$ , very light dark matter particles will have such a small rate of annihilation that their relic density will be much larger than the observed relic density of dark matter. However, Boehm and Fayet [19] showed that the Lee-Weinberg limit can be evaded with a light scalar dark matter candidate  $\chi$  interacting with a new light gauge boson  $U$  and a new heavy fermion  $F$ , both of which have very weak coupling to ordinary matter.

The introduction of these two new mediator particles resolves the issue of reconciling a large annihilation cross-section in the early universe with a small cross-section today, to avoid overproduction of low-energy gamma rays. The two possible annihilation channels of the dark matter particle  $\chi$  (and its antiparticle  $\chi^*$ ) to  $e^+e^-$  are shown in figure 1. Indeed, the annihilation cross-section through a  $U$  boson is purely velocity-dependent, while the  $F$ -exchange cross-section has both a velocity-dependent and a velocity-independent piece, so the  $U$ -mediated annihilation is suppressed by several orders of magnitude today because the dark matter velocity is so small. Boehm *et al.* showed in 2006 [20] that the phenomenological and astrophysical constraints on this model can be accommodated by assuming that the  $U$ -mediated annihilation sets the relic density of dark matter, while the  $F$ -mediated annihilation controls the present-day rate of annihilation, and is responsible for the INTEGRAL signal. In particular, the INTEGRAL results cannot be explained with a  $U$  boson alone, nor can they be explained if  $\chi$  is a fermion. While a variation on this model has been proposed [21] where the  $U$  is replaced by a neutral fermion  $N$  which only couples to  $\chi$  and neutrinos, this work will focus on the model with the  $U$ .

The original model placed the dark matter mass  $m_\chi$  anywhere from 1 to 100 MeV, but subsequent consideration by Beacom and Yüksel [22] of the effects of the interstellar medium on the positrons produced in the annihilation reaction placed a stringent upper

bound on  $m_\chi$ . If positrons are produced in the galactic center, they will produce photons as they propagate by both bremsstrahlung and in-flight annihilation with electrons in the interstellar medium. By examining the measured spectrum of MeV gamma rays from the galactic center and comparing with the number of positrons inferred from the INTEGRAL data, Beacom set an upper limit of 3 MeV on the energy of the injected positrons. This constraint can be relaxed to 7.5 MeV for different assumptions about the ionization state of the interstellar medium [23], but this bound is extremely robust because it makes no reference to any particular model of dark matter.

The lower bound on  $m_U$ ,  $m_U > m_\chi$ , can be obtained [23] by noting that if  $m_U < m_\chi$ , the principal annihilation mechanism is  $\chi\chi \rightarrow UU$  through a  $t$ -channel  $\chi$ , since the  $U - \chi - \chi$  coupling is expected to be much larger than the  $U - e - e$  coupling. Not only would this invalidate Boehm *et al.*'s requirement of a velocity-suppressed cross-section, but it would keep the  $\chi$  and  $U$  in thermal equilibrium in the early universe, and the number density of the heavier  $\chi$  would be so suppressed compared to the  $U$  that it could no longer serve as a dark matter candidate. Additionally, a lower bound on  $m_F$  can be obtained by noting that since the  $F$  is charged, its mass is constrained to be above 100 GeV by LEP data [24].

By matching the cross-sections of  $U$ - and  $F$ -mediated annihilations to the observed relic density of dark matter and the INTEGRAL flux, respectively, and assuming that the  $\chi$  can only decay into  $e^+e^-$ , one obtains the relations [20, 25]

$$\frac{m_F}{100 \text{ GeV}} \simeq 6 \times 10^3 \frac{c_l c_r}{m_\chi/\text{MeV}} \quad (1)$$

$$|C_\chi f^e| \simeq 10^{-6} \frac{m_U^2 - 4m_\chi^2}{m_\chi(1.8 \text{ MeV})} \quad (2)$$

where  $c_l$  and  $c_r$  are the  $F - \chi - e_L$  and  $F - \chi - e_R$  couplings,  $C_\chi$  is the  $U - \chi - \chi$  coupling, and  $f^e$  is the  $U - e - e$  coupling. These constraints make a direct observation of either the  $U$  or  $F$  quite difficult. Strictly speaking, there is no upper bound on  $m_F$ , and even if  $c_l, c_r < 1$  are required,  $m_F$  can be as large as 10 TeV. Eq. (2) shows that, for  $C_\chi \approx 1$ ,  $f^e$  must be extremely small, and any experiment to produce a  $U$  must compete with significant higher-order QED backgrounds.

## 3.2 Signatures from pion decay

Rather than trying to observe the  $U$  or  $F$  directly, one can search for their effects in low-energy physics. For example, Boehm and Silk [26] recently proposed a search for the  $F$  in precision data on the electron anomalous magnetic moment. Along these lines, one can ask if the distinctive phenomenology of the  $U$  could also appear in low-energy physics. In particular, the massive  $U$  has a longitudinal polarization state which the massless photon lacks. Thus, the rare decay  $\pi^0 \rightarrow \gamma^* \rightarrow e^+e^-$ , which is forbidden at tree level in QED because the pion is a pseudoscalar and the photon has no spin-0 state, could be enhanced by the process  $\pi^0 \rightarrow U^* \rightarrow e^+e^-$ . This scenario, which was published as [27], is reviewed below.

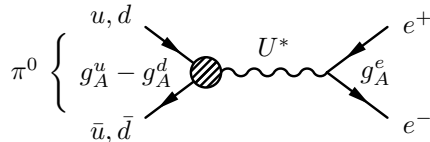


Figure 2: *Feynman diagram for  $\pi^0 \rightarrow e^+e^-$ .*

The decay  $\pi^0 \rightarrow \gamma^* \rightarrow e^+e^-$  has been studied extensively since the 1960's [28], since its extremely small branching ratio makes it sensitive to the effects of new physics. The lowest-order diagram has a two-photon intermediate state, so it is suppressed relative to the dominant decay channel  $\pi^0 \rightarrow \gamma\gamma$  by a factor of  $\alpha^2$ , and helicity conservation suppresses it further by  $(m_e/m_\pi)^2$ . The most recent measurement of the branching ratio was by KTeV [29], which found

$$B^{\text{meas}}(\pi^0 \rightarrow e^+e^-) = (7.48 \pm 0.29 \pm 0.25) \times 10^{-8}$$

after extrapolating from the selected events to the entire allowed kinematic region. The most recent theoretical estimate for this branching ratio is [30]

$$B^{\text{SM}}(\pi^0 \rightarrow e^+e^-) = (6.2 \pm 0.1) \times 10^{-8} .$$

This result was obtained with the operator product expansion in QCD and using data from the CLEO experiment to constrain the pion transition form factor for  $\pi^0 \rightarrow \gamma^*\gamma^*$ , and agrees with derivations using other QCD approximation schemes (sum rules, vector meson dominance, and the nonlocal quark model) to within the quoted uncertainties. However, this theoretical result is  $3\sigma$  below the measured value, which suggests that new physics may be responsible for the excess in the branching ratio.

We can interpret the excess,  $B^{\text{meas}} - B^{\text{SM}} = (1.3 \pm 0.4) \times 10^{-8}$ , in the context of the light dark matter model. We extend the model by assuming that the  $U$  couples to first-generation quarks as well as electrons, and allow for these couplings to have both vector and axial components, so that the interaction Lagrangian is

$$\begin{aligned} \mathcal{L}_{int} = & U_\mu \{ \bar{u}\gamma^\mu (g_V^u + \gamma_5 g_A^u) u + \bar{d}\gamma^\mu (g_V^d + \gamma_5 g_A^d) d \\ & + \bar{e}\gamma^\mu (g_V^e + \gamma_5 g_A^e) e \} . \end{aligned} \quad (3)$$

We will further assume that the couplings to second- and third-generation fermions are suppressed. The full lowest-order amplitude for the process  $\pi^0 \rightarrow e^+e^-$  is a sum of the standard model amplitude  $\mathcal{M}_{SM}$  and the tree-level diagram  $\mathcal{M}_U$ , shown in figure 2.  $\mathcal{M}_{SM}$  can be obtained from [30]:

$$\mathcal{M}_{SM} = (2m_\pi m_e) A e^{i\delta}; \quad A = (2.9417 \times 10^{-7}/\text{MeV}), \quad \delta = -1.05125 \quad (4)$$

where the relative phase  $\delta$  is found by comparing the magnitude of  $\mathcal{M}_{SM}$  with the imaginary part in equation (5) of [30].  $\mathcal{M}_U$  is computed by modeling the pion vertex with a form factor

$F^\mu = f_\pi p^\mu$ , where  $p^\mu = p_{e^+}^\mu + p_{e^-}^\mu$  is the momentum of the pion and  $f_\pi$  is the pion decay constant.

It turns out that the only combination of couplings which contributes to this decay is  $g_A^u - g_A^d$ . To see this, note that the matrix element for the decay process will be proportional to the matrix element which couples the pion to the QCD vacuum through the  $U$  boson,

$$\langle 0 | \bar{u} \gamma^\mu (g_V^u + \gamma^5 g_A^u) u + \bar{d} \gamma^\mu (g_V^d + \gamma^5 g_A^d) d | \pi^0 \rangle.$$

However, since the pion is a pseudoscalar, purely vector terms such as  $\langle 0 | \bar{u} \gamma^\mu g_V^u u | \pi^0 \rangle$  vanish because the QCD vacuum is parity-even, and only purely axial terms remain. Furthermore, the pion state is  $|\pi^0\rangle = \frac{1}{\sqrt{2}}(|u\bar{u}\rangle - |d\bar{d}\rangle)$ , so the quark couplings must enter in the combination  $g^u - g^d$ . Thus, the full matrix element is

$$\mathcal{M} = [\bar{u} \gamma^\mu v] \frac{(g_A^u - g_A^d) g_A^e}{m_\pi^2 - m_U^2} \left[ g_{\mu\nu} - \frac{p_\mu p_\nu}{m_U^2} \right] f_\pi p^\nu \quad (5)$$

where  $u$  and  $v$  are the electron and positron spinors, respectively. Note that the coupling at the electron vertex is also purely axial; if the  $U$  boson acquires its mass from a  $U(1)$  gauge symmetry which is spontaneously broken, its longitudinal mode will be a pseudoscalar, with axial couplings to electrons. Because the pion is a pseudoscalar, only the longitudinal mode contributes to the decay. In the original dark matter model, relic density considerations do not constrain the nature of the electron coupling to be either vector or axial, although such constraints may come from other low-energy phenomenology, as will be discussed below. For an on-shell pion,  $p^\mu p_\mu = m_\pi^2$ , with the result

$$\mathcal{M} = \frac{(g_A^d - g_A^u) g_A^e f_\pi}{m_U^2} [\bar{u} \gamma^\mu v] p_\mu. \quad (6)$$

The partial width for  $\pi^0 \rightarrow e^+ e^-$  is given by [31]

$$\Gamma = \frac{|\vec{p}|}{8\pi m_\pi^2} |\mathcal{M}_{SM} + \mathcal{M}_U|^2, \quad (7)$$

where the total matrix element on the left is summed over final electron and positron spins, and  $|\vec{p}|$  is the momentum of one of the outgoing particles, approximately equal to  $m_\pi/2$  if the electron mass is neglected. In terms of the magnitude and phase of  $\mathcal{M}_{SM}$ ,

$$\Gamma = \frac{m_\pi m_e^2}{2\pi} \left( A^2 + 2A \cos \delta \frac{(g_A^u - g_A^d) g_A^e f_\pi}{m_U^2} + \frac{(g_A^u - g_A^d)^2 (g_A^e)^2 f_\pi^2}{m_U^4} \right) \quad (8)$$

The smallness of the SM branching ratio makes the last two terms comparable in size, despite the fact that the last term carries extra factors of the  $U$  boson mass and couplings. Plugging in the known experimental values  $f_\pi = 130 \pm 5$  MeV and  $\tau_{\pi^0} = 1/\Gamma_{tot} = (84 \pm 6) \times 10^{-18}$  s [24] gives a relation between  $m_U$  and the coupling constants,

$$\frac{(g_A^u - g_A^d) g_A^e}{m_U^2} = (4.0 \pm 1.8) \times 10^{-10} \text{ MeV}^{-2}. \quad (9)$$

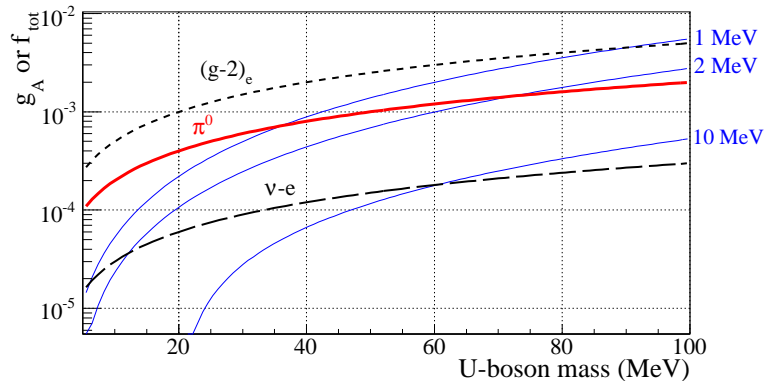


Figure 3: Constraints on the couplings as a function of  $m_U$ . The thick (red) line labeled “ $\pi^0$ ” shows the result Eq. (10). The short-dashed line comes from constraints on  $(g-2)_e$  [25], the long-dashed line comes from constraints on  $\nu - e$  scattering [25], and the solid (blue) lines labeled with “ $n$  MeV” are based on relic density calculations [25].

To make contact with the other constraints on the dark matter model, consider the case where  $g_A^u - g_A^d = g_A^e \equiv g_A$ . Although this is an arbitrary choice, such a relation might be expected to hold within an order of magnitude, as it does in QED where the couplings are interpreted as electric charges. In this case, one finds

$$g_A = 2.0_{-0.5}^{+0.4} \times 10^{-4} \times \left( \frac{m_U}{10 \text{ MeV}} \right) \quad (10)$$

where the asymmetric error bars come from taking the square root of (9). This constraint is shown in figure 3 as a thick line labeled “ $\pi^0$ ”. The solid blue lines in figure 3 come from (2), assuming  $C_\chi = 1$ , and are labeled by the mass of the dark matter particle  $\chi$  in MeV. For a given  $m_\chi$ , these lines mark the maximum possible value of the total coupling  $f_{tot}^e = \sqrt{(f_V^e)^2 + (f_A^e)^2}$ . If we assume a purely axial coupling  $f_A^e$ , the short-dashed line labeled  $(g-2)_e$  constrains this coupling  $f^e$  based on measurements of the electron anomalous magnetic moment [25]. In general, it is not possible to constrain the axial and vector couplings separately, but we note that the axial coupling constraint is stronger, and yet lies safely above the pion constraint for all values of  $m_U$ . The long-dashed line labeled  $\nu - e$  is a constraint on  $f_{tot}$  resulting from data on  $\nu - e$  scattering, assuming the  $U - \nu$  coupling is similar to the  $U - e$  coupling; this relatively severe constraint can be avoided if we assume that the coupling of the  $U$  to electrons is mostly right-handed. As can be seen from the figure, this constraint would rule out the dark matter model entirely except for the very smallest values of  $m_U$ . Similarly, rather strong constraints on the axial coupling to quarks coming from heavy quarkonium decays [25] can be avoided if we assume, as stated earlier, that the coupling to second- and third-generation fermions is suppressed.

If we now identify the  $g_A^e$  in this pion decay scenario with the  $f^e$  of Eq. (2), we see that the couplings are constrained by pion decay in roughly the same way as by the relic

density constraints. This is remarkable because  $\mathcal{M}_U$  depends on a different set of couplings and experimental input than the light dark matter model; these new constraints provide a different view of the phenomenology of the light  $U$  boson. In particular, since the pion decay singles out the axial coupling to electrons, an experimental confirmation of the light dark matter model could provide the separation of axial and vector couplings which is not possible by examining the electron  $g - 2$  alone.

## 4 Bound states of heavy dark matter

### 4.1 Formalism

Moving from light dark matter to heavy dark matter, in this section models of dark matter will be considered whose phenomenology is governed by the possibility of forming bound states. In particular, consider the case of a complex scalar dark matter particle interacting with a scalar mediator:

$$\mathcal{L} = (\partial_\mu \chi)(\partial^\mu \chi^*) - M^2 \chi \chi^* + \frac{1}{2}(\partial_\mu \phi)^2 - \frac{1}{2}m^2 \phi^2 + A\phi \chi \chi^* \quad (11)$$

Here,  $M$  is the mass of the  $\chi$  WIMP,  $m$  is the mass of the  $\phi$  mediator, and  $A$  is the coupling between the  $\chi$  and the  $\phi$ , with dimensions of mass. Since  $\chi$  is complex, there are both WIMPS  $\chi$  and anti-WIMPS  $\bar{\chi}$ . The key feature of this model is the scalar mediator, which results in a *universally attractive* force [32]; not only can  $\chi\bar{\chi}$  bound states form, but  $\chi\chi$  and  $\bar{\chi}\bar{\chi}$  can form as well. The force between two WIMPS is described by a Yukawa potential,

$$V(r) = -\frac{\alpha_\chi}{r} e^{-mr}, \quad (12)$$

where  $\alpha_\chi = |A|^2/4\pi M^2$ . In general,  $M$  will be TeV-scale,  $m$  will be GeV-scale, and  $\alpha_\chi$  will be assumed to be less than 1 so as to keep the theory perturbative. However, for the particular case of a scalar WIMP coupled to a scalar mediator, the theory may still be perturbative if  $\alpha \lesssim 4\pi$  because of one-loop corrections to scattering amplitudes. To relate this model to the INTEGRAL signal, one can assume that the only interactions of the dark matter sector with the Standard Model are Yukawa couplings of the  $\phi$  to electrons and positrons,

$$\mathcal{L}_{DM-SM} = g_e \phi \bar{e} e. \quad (13)$$

The constraints on the coupling constant  $g_e$  depend on  $m$ ; for  $m = 1$  GeV,  $g_e$  must be less than  $10^{-3}$  or so to be consistent with the absence of signatures for such particles at  $e^+/e^-$  colliders [24], but for heavier  $\phi$ ,  $g_e$  is somewhat less constrained.

The spectrum of bound states of a Yukawa potential shows some interesting features not present in the Coulomb case. Most importantly, for any value of the coupling  $\alpha_\chi$ , there are only finitely many bound states, in contrast to the infinite number of bound states of the Coulomb potential. Qualitatively, this arises from the exponential suppression of the potential for  $r \gg 1/m$ . In addition, there is no degeneracy in the orbital quantum number

$l$ , because the accidental symmetry peculiar to the Coulomb potential is no longer present. Both these features can be seen quantitatively by solving the non-relativistic Schrodinger equation numerically. This calculation was first done in 1970 [33] to model the screening of the Coulomb potential in many-electron atoms; although Rogers *et al.* only presented certain points in parameter space in their results, their methods are easily applied to find the energy eigenvalues and construct the radial wavefunctions anywhere in the parameter space.

The behavior of the bound state spectrum can be captured by defining the quantity

$$D := \frac{\alpha_\chi M}{2m}, \quad (14)$$

and writing the energy spectrum as

$$E(n, l) = \frac{\alpha_\chi^2 M}{4} \epsilon(n, l). \quad (15)$$

Note that, making an analogy with the hydrogen atom, the prefactor in Eq. (15) is the reduced-mass Rydberg constant for the WIMP-WIMP system. As  $D \rightarrow \infty$ , or equivalently as  $m \rightarrow 0$ , the potential approaches a Coulomb potential, and  $\epsilon(n, l) \rightarrow 1/n^2$ , as expected for the Coulomb spectrum. The existence of a  $1s$  bound state requires  $D > 0.82$ , and a  $2s$  bound state requires  $D > 3.2$ .

In this model, transitions among bound states, or transitions between the continuum and the bound states, will act as sources for galactic positrons. The simplest possibilities are the formation of the ground state from free WIMPS, or the transition  $2s \rightarrow 1s$ ; both processes result in the emission of an off-shell  $\phi$ , which will eventually decay into  $e^+/e^-$ . If the energy of the transition is small enough, electrons and positrons are the only possible SM decay products, as long as the  $\phi$  doesn't couple to photons; decays to  $\nu\bar{\nu}$  are forbidden by angular momentum conservation, since  $\chi$  and the  $1s$ ,  $2s$  bound states are scalars. In fact, as explained in the section on light dark matter, this constraint on the transition energy is satisfied because positrons produced in the galactic center are constrained to have injection energies less than about 5 MeV, so the regions of parameter space of interest satisfy either  $E(1, 0) \lesssim 10$  MeV or  $E(1, 0) - E(2, 0) \lesssim 10$  MeV. This second condition is extremely restrictive, for the following reason. Since  $D = \alpha_\chi M/2m > 3.2$  for a  $2s$  state,  $D$  is sufficiently large that  $\epsilon(1, 0) - \epsilon(2, 0)$  is  $O(1)$ ; that is, the potential behaves similarly to a Coulomb potential for the ground state. Requiring  $E(2, 0) - E(1, 0) \approx \alpha_\chi^2 M/4 < 10$  MeV gives  $m\alpha_\chi \lesssim 6$  MeV, so either a very small coupling or a very light  $\phi$  is necessary. On the other hand, the condition  $E(1, 0) \lesssim 10$  MeV is much less restrictive, so we focus on this case first.

## 4.2 $\Psi_{1s}$ production

We imagine that the galactic dark matter is a mixture of free WIMPS and WIMP-WIMP  $1s$  bound states (notated  $\Psi$ ), whose relative proportions are fixed by tracking the behavior of WIMPS in the early universe as they freeze out from the SM. For now, we simply investigate

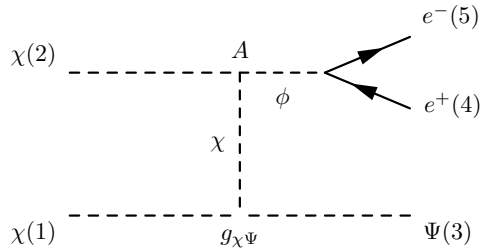


Figure 4: *Feynman diagram for  $\Psi$  production.*

whether the model is viable when the relic fraction of bound states is negligibly small, so that all WIMPS are free. The cross-section for the reaction  $\chi\chi \rightarrow \Psi\phi$  (where  $\phi$  decays to  $e^+/e^-$  with unit probability) can be related to the flux of galactic positrons by averaging the cross-section over the velocity distribution of WIMPS and the galactic dark matter profile. This calculation was done by Finkbeiner *et al.* [34] using the Einasto profile [35], with the result

$$\Phi \approx 3 \times 10^{42} \frac{e^+}{\text{sec}} \left( \frac{\langle \sigma v \rangle}{2 \times 10^{-20} \text{ cm}^3 \text{ s}^{-1}} \right) \left( \frac{500 \text{ GeV}}{M} \right)^2. \quad (16)$$

Here,  $\sigma$  is the cross-section for  $\Psi$  production,  $v$  is the relative velocity of the WIMPS, and the brackets denote thermal averaging. The final factor originates from knowing only the energy density of dark matter, and not the number or mass of the particles; lighter particles implies more particles necessary to make up the required energy density, and hence more scattering centers. The  $\Psi$ -formation model will be a viable explanation of the INTEGRAL signal if it can reproduce the value  $2 \times 10^{-20} \text{ cm}^3 \text{ s}^{-1}$  for the cross-section times relative velocity with a 500 GeV WIMP.

The Feynman diagram for the process  $\chi\chi \rightarrow \Psi e^+ e^-$  is shown in figure 4. Since the  $\Psi$  is a composite particle, the  $\chi - \chi - \Psi$  vertex is an effective one, with an effective coupling  $g_{\chi\Psi}$  related to the overlap between the  $1s$  radial wavefunction and the incoming plane wave states. The 4-momentum of the emitted  $\phi$  is  $q_1 = p_1 + p_2 - p_3$  and the momentum of the  $t$ -channel  $\chi$  is  $q_2 = p_3 - p_1$ , or  $p_3 - p_2$  for the crossed diagram, where the  $\phi$  is emitted from the  $\chi$  with momentum  $p_1$ . The total matrix element, obtained by summing these two diagrams, is:

$$\mathcal{M} = [\bar{u}(5)v(4)] \frac{1}{q_1^2 - m^2} A \left( \frac{1}{(p_3 - p_2)^2 - M^2} + \frac{1}{(p_3 - p_1)^2 - M^2} \right) g_{\chi\Psi}, \quad (17)$$

where  $\bar{u}$  is the electron spinor and  $v$  is the positron spinor. In the CM frame,  $q_1 \approx 2M - m_\psi =: E_B$ , the binding energy of the  $\Psi$ , which must be less than 10 MeV. So  $q_1^2 - m^2 \approx -m^2$ . The

second denominator can be approximated as follows:

$$\begin{aligned}
(p_3 - p_2)^2 - M^2 &= m_\psi^2 + M^2 - 2(E_2 E_3 - \vec{p}_2 \cdot \vec{p}_3) - M^2 \\
&\approx m_\psi^2 - 2M m_\psi \\
&= (2M - E_B)^2 - 2M(2M - E_B) \\
&\approx -2M E_B
\end{aligned}$$

The second line follows from the fact that the incident  $\chi$ 's are non-relativistic; the average velocity of dark matter in our galaxy is about  $10^{-3} c$ . The same approximation holds for  $(p_3 - p_1)^2$ . The spinor contribution to  $\langle |\mathcal{M}|^2 \rangle$  is  $\text{tr}[(p_5^\mu \gamma_\mu + m_e)(p_4^\mu \gamma_\mu - m_e)] = 4(p_4 \cdot p_5 - m_e^2)$ . So finally,

$$\langle |\mathcal{M}|^2 \rangle = \frac{4A^2 g_{\chi\Psi}^2}{m^4 M^2 E_B^2} (p_4 \cdot p_5 - m_e^2) \quad (18)$$

Note that both  $A$  and  $g_{\chi\Psi}$  have dimensions of mass.

The differential cross-section for a  $2 \rightarrow 3$  process is given by the Golden Rule [31]:

$$d\sigma = \langle |\mathcal{M}|^2 \rangle \frac{1}{4\sqrt{(p_1 \cdot p_2)^2 - m_1^2 m_2^2}} \frac{1}{(2\pi)^9 2^3 E_3 E_4 E_5} (2\pi)^4 \delta^4(p_1 + p_2 - p_3 - p_4 - p_5) d^3 \vec{p}_3 d^3 \vec{p}_4 d^3 \vec{p}_5 \quad (19)$$

In the CM frame,  $\sqrt{(p_1 \cdot p_2)^2 - m_1^2 m_2^2} = (E_1 + E_2) |\vec{p}_1| \approx 2M |\vec{p}_1|$ , and  $E_3 \approx m_\psi \approx 2M$ . The delta function splits as  $\delta(E_{tot} - E_3 - E_4 - E_5) \delta^3(\vec{p}_3 + \vec{p}_4 + \vec{p}_5)$ , and performing the  $p_3$  integral sets  $\vec{p}_3 = -(\vec{p}_4 + \vec{p}_5)$ .

The  $p_4$  and  $p_5$  integrals can be approximated as follows. The purpose of the remaining delta function is to set the limits of integration on whichever momentum remains to be integrated over; this can be done by hand by dropping the delta function, integrating up to  $|\vec{p}_{max}| \approx E_B/2$ , and pulling out a factor of  $\frac{1}{|\vec{p}_5|}$  for dimensional consistency. So

$$\begin{aligned}
&\int \int \frac{p_4 \cdot p_5 - m_e^2}{E_4 E_5} d^3 \vec{p}_4 d^3 \vec{p}_5 \longrightarrow 4\pi \int_0^{|\vec{p}_{max}|} \left(1 - \frac{\vec{p}_4 \cdot \vec{p}_5 + m_e^2}{E_4 E_5}\right) |\vec{p}_5| d|\vec{p}_5| \int d^3 \vec{p}_4 \\
&= 8\pi^2 \int_0^{|\vec{p}_{max}|} \left(1 - \frac{|\vec{p}_4| |\vec{p}_5| \cos \theta + m_e^2}{E_4 E_5}\right) |\vec{p}_5| d|\vec{p}_5| \int_0^{|\vec{p}_{max}|} |\vec{p}_4|^2 d|\vec{p}_4| \int_0^\pi \sin \theta d\theta \\
&= 8\pi^2 \int_0^{|\vec{p}_{max}|} \int_0^{|\vec{p}_{max}|} \left(1 - \frac{m_e^2}{E_4 E_5}\right) |\vec{p}_4|^2 |\vec{p}_5| d|\vec{p}_4| d|\vec{p}_5| \\
&\qquad\qquad\qquad \approx 16\pi^2 \frac{|\vec{p}_{max}|^5}{6}, \quad (20)
\end{aligned}$$

where the last line follows from dropping the term proportional to  $m_e^2$ , which is suppressed relative to the remaining term by a factor of  $m_e^2/|\vec{p}_{max}|^2 \approx 10^{-2}$ . So, the final expression for

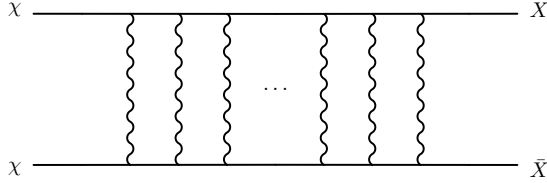


Figure 5: *Ladder diagram giving rise to the Sommerfeld enhancement. Figure from [36].*

the total cross-section is

$$\begin{aligned}
 \sigma_{tot} &\approx \frac{4A^2 g_{\chi\Psi}^2}{m^4 M^2 E_B^2} \frac{1}{8M|\vec{p}_1|} \frac{1}{32\pi^5 \cdot 8(2M)} 16\pi^2 \frac{|\vec{p}_{max}|^5}{6} \\
 &= \frac{|\vec{p}_{max}|^5 A^2 g_{\chi\Psi}^2}{384\pi^3 m^4 M^2 E_B^2 |\vec{p}_1|} \times (0.39 \text{ GeV}^2 \cdot \text{mbarn})
 \end{aligned} \tag{21}$$

Now, put  $A = g_{\chi\Psi} = \sqrt{4\pi\alpha_\chi} M$ ; in fact,  $g_{\chi\Psi}$  will be smaller than this because the wavefunction overlap is necessarily less than 1, but this approximation provides a good upper bound on the cross-section without requiring detailed numerical integration. Approximating  $\langle\sigma v\rangle$  using a flat velocity distribution and using  $|\vec{p}_1| \approx Mv$ , the multiplication by  $v_{rel} = 2v$  cancels the  $v$  in the denominator and leaves  $2/M$ . Replacing  $|\vec{p}_{max}|$  by  $E_B/2$  and setting  $E_B = 10 \text{ MeV}$  in Eq. (21), the result is

$$\sigma v \approx \frac{\alpha_\chi^2}{m^4 M} \times (1.2 \times 10^{-27} \text{ GeV}^5 \text{ cm}^3/\text{sec}) \tag{22}$$

This cross-section is several orders of magnitude too small to explain INTEGRAL, for reasonable values of  $\alpha_\chi$ ,  $m$ , and  $M$ . This is not quite the end of the story, though, because the low incident WIMP velocities allow for the possibility of a Sommerfeld enhancement, a nonperturbative effect which can enhance the cross-section significantly for certain values of the masses and couplings. In quantum field theory, this effect arises through multiple exchanges of the mediator particle, as shown in the “ladder diagram” of figure 5; this is equivalent to solving the non-relativistic Schrodinger equation with plane-wave boundary conditions at infinity. It turns out that an enhancement of the cross-section by a factor of  $10^6$  is possible if  $M \approx 2m/\alpha_\chi$  [36]; for a 500 GeV WIMP, this fixes  $m = \alpha_\chi \cdot 250 \text{ GeV}$ . Comparing with the Finkbeiner cross-section gives  $\alpha_\chi = 1.8 \times 10^{-7}$  and  $m = 0.045 \text{ MeV}$ , which are clearly unreasonable values. Unfortunately, it appears that this simple model cannot explain the INTEGRAL results.

### 4.3 $2s \rightarrow 1s$ transitions

Despite the restricted parameter space in the model of  $2s \rightarrow 1s$  transitions, as described in section 4.1, the cross-section for the upscattering process which produces the  $2s$  excited states does not suffer from the same large suppressions as the  $\Psi$  production cross-section,

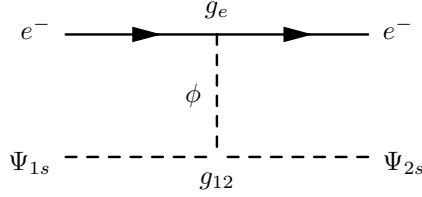


Figure 6: *Feynman diagram for  $\Psi_{1s} - \Psi_{2s}$  transitions.*

so this scenario merits a second look. Now, we imagine that all but a negligible fraction of WIMPS are in  $1s$  bound states, which can be excited to the  $2s$  state by interacting with an incident electron. This process is shown in figure 6. The  $\Psi_{2s}$  will then decay by spontaneous emission of a  $\phi$ . Because the process  $e^- + \Psi_{1s} \rightarrow e^- + \Psi_{2s}$  is a  $2 \rightarrow 2$  process, the cross-section will be larger than the  $2 \rightarrow 3$  process by phase-space considerations alone; additionally, the  $\chi$  never goes off-shell, further enhancing the cross-section relative to  $\Psi$  production. However, the small coupling  $g_e$  of the  $\phi$  to electrons now plays a significant role, as does the number density and energy spectrum of medium-energy electrons at the center of the galaxy.

In calculating the cross-section, note that once again, the  $\phi - \Psi_{1s} - \Psi_{2s}$  is an effective vertex, with an effective coupling given by  $g_{12}$ , which has dimensions of mass. The calculation of the matrix element is straightforward:

$$\mathcal{M} = g_e[\bar{u}(3)u(1)]\frac{1}{q^2 - m^2}g_{12} \quad (23)$$

The spinors now contribute a factor of  $\text{tr}[(p_1^\mu\gamma_\mu + m_e)(p_3^\mu\gamma_\mu + m_e)] = 4(p_1 \cdot p_3 + m_e^2)$ ; averaging over initial spins gives a factor of  $1/2$ , so

$$\langle |\mathcal{M}|^2 \rangle = \frac{2g_e^2 g_{12}^2 (p_1 \cdot p_3 + m_e^2)}{(q^2 - m^2)^2} \quad (24)$$

The calculation of the cross-section is most easily performed in the lab frame, since the slow-moving WIMPS are essentially at rest compared to the incident relativistic electrons. Let  $E$  be the energy of the incident electron,  $E'$  the energy after upscattering, and  $E_{12}$  the transition energy between the  $\Psi_{1s}$  and the  $\Psi_{2s}$ . The two phase-space integrals for this  $2 \rightarrow 2$  process are both integrals over delta functions, which are trivial, and the Golden Rule immediately yields an expression for the cross-section:

$$\sigma(E) = \frac{g_e^2 g_{12}^2}{256\pi E^2 M^2} \left( \ln \frac{m^2 + 2E(E' + |\vec{p}_3|)}{m^2 + 2E(E' - |\vec{p}_3|)} - \frac{4m^2 E |\vec{p}_3|}{(m^2 + 2E(E' - |\vec{p}_3|))(m^2 + 2E(E' + |\vec{p}_3|))} \right), \quad (25)$$

where  $E' \approx E - E_{12}$  and  $|\vec{p}_3| = \sqrt{E'^2 - m_e^2}$ . To arrive at this expression, similar approximations were made to those in section 4.2: dropping the electron mass, putting  $M_{\Psi_{1s}} = M_{\Psi_{2s}} = 2M$ , etc.

The energy spectrum of electrons in the galactic center can be modeled by a power law, with varying exponent in different energy ranges;  $N(E) \propto E^{-1.6}$  for  $10 \text{ MeV} < E < 1 \text{ GeV}$ ,

while  $N(E) \propto E^{-2.8}$  for  $1 \text{ GeV} < E < 10 \text{ GeV}$  [37]. Since the energy spectrum drops sharply at  $E = 1 \text{ GeV}$ , and the cross-section begins to be suppressed by higher powers of  $E$  at this energy for  $m \sim 1 \text{ GeV}$ , it suffices to integrate the cross-section up to energies of  $1 \text{ GeV}$ . The result is

$$\langle \sigma v \rangle = \frac{g_e^2 g_{12}^2}{M^2} (2.9 \times 10^{-20} \text{ cm}^3 \text{ s}^{-1}) \quad (26)$$

for  $m = 1 \text{ GeV}$ . Now, using the normalization  $N_0 = 2.5 \times 10^3 \text{ particles m}^{-3}$  [37] for the electron energy spectrum, and a model for the density of dark matter at the galactic center, the flux of positrons can be calculated. As an example, consider an NFW profile [38], which is simply a power law  $\rho(r) = C/r$  in the innermost kiloparsec of the galaxy, which is the extent of the INTEGRAL signal [39]. The normalization is fixed by matching the full NFW profile to the local density of DM:  $C = \rho_0 r_0$ , where  $\rho_0 = 0.347 \text{ GeV cm}^{-3}$  and  $r_0 = 16.7 \text{ kpc}$  [20]. Thus, the positron flux is

$$\Phi = \int_0^{r_c} 4\pi r^2 \langle \sigma v \rangle \frac{\rho(r)}{m_\Psi} N_0 dr, \quad (27)$$

where  $r_c \sim 1 \text{ kpc}$  is the maximum radius of the INTEGRAL signal. Matching this with the observed flux, and once again using  $A = \sqrt{4\pi\alpha_\chi} M$  as an order-of-magnitude estimate, gives the condition

$$\frac{\alpha_\chi g_e^2}{M} = 6.1 \times 10^{-3} \text{ GeV}^{-1} \quad (28)$$

for  $m = 1 \text{ GeV}$ . Comparison with Eq. (22) shows that the scenario of  $1s - 2s$  transitions is pushed to the same small corner of parameter space as the original model of section 4.2; despite the larger cross-section, the necessarily small value of  $g_e \sim 10^{-3} - 10^{-4}$  makes an explanation of the INTEGRAL flux difficult without an extremely light  $\chi$ , which would have the wrong annihilation cross-section to explain the observed relic density. Recalling the condition  $m\alpha_\chi \lesssim 6 \text{ MeV}$  for the existence of a  $2s$  bound state, though, we can try to dial the  $\phi$  mass down to very small values in the hopes of both enhancing the cross-section and keeping  $\alpha_\chi$  relatively large. Even for  $m = 50 \text{ MeV}$  and  $\alpha_\chi = 0.01$ , though,  $g_e$  would need to be of order 1 to explain INTEGRAL, in clear violation of collider bounds on light  $Z'$ -like particles.

## 5 Conclusion

The considerations of the WIMP bound state model illustrate the principal difficulty of explaining the INTEGRAL data: the flux of positrons from the galactic center is fantastically large. Conventional models of astrophysical phenomena have difficulty accounting for this large value, which is why the data have resisted explanation for so long, and particle-physics models tend to suffer from too small a positron production cross-section while still maintaining the correct relic density of dark matter. However, the model of light dark matter by Boehm *et al.* is able to correctly reproduce both the flux and the relic density by the fortunate confluence of a velocity-dependent cross-section and an abundance of scattering centers due to the very small dark matter mass. Although this model has been constrained

and revised considerably since its proposal, it has certainly not yet been ruled out, and in fact possibilities exist for its confirmation in low-energy physics. In particular, under certain additional assumptions about the  $U$  boson coupling to first-generation quarks, the light dark matter model can explain a  $3\sigma$  excess in rare pion decays in a manner which is consistent with other independent astrophysical constraints.

While the models for WIMP bound states considered above fail to explain INTEGRAL, other models of TeV-scale dark matter with GeV-scale mediators succeed by postulating an excited dark matter state whose mass splitting is controlled by a broken gauge symmetry [34]. These models also have the attractive feature of potentially explaining the excess of GeV galactic positrons observed by the PAMELA experiment [40], and the keV-scale annual modulation signal observed by the DAMA experiment [41]. One possible avenue for future research on WIMP bound states would be to consider strongly-coupled systems, with  $\alpha_\chi > 4\pi$ ; instead of an analogy with the weakly-bound hydrogen atom, the WIMP-WIMP bound state would be analogous to the proton or neutron, with excited states the analogs of the  $\Delta$  particles. The mass splittings would then be controlled by a hyperfine-like interaction, which could avoid the severe constraints placed on the masses and couplings by requiring several bound states for the weakly-coupled Yukawa potential. Taking advantage of the much larger cross-section for upscattering transitions described in section 4.3, and the fact that a strong coupling would likely push the relic fraction of bound states over free WIMPS to unity, an explanation of the INTEGRAL 511 keV signal could still be possible in the context of this model.

## Acknowledgements

I would like to thank Professor Michael Schmitt for giving me my first research project my freshman year, and leading me into the exciting world of high-energy physics and phenomenology. Thank you also to the many professors who have helped me in my research through fruitful discussions, including Mayda Velasco, André de Gouvêa, Vicky Kalogera, and Ian Low. Finally, thank you to my advisor, Professor Tim Tait, for all his advocacy, and for putting up with an undergraduate's hectic schedule which unfortunately leaves too little time for research.

## References

- [1] W.J.G. de Blok and S. McGaugh. The dark and visible matter content of low surface brightness disc galaxies. *Mon. Not. R. Astron. Soc.*, 290:533, 1997.
- [2] D. Clowe and M. Bradac et al. A direct empirical proof of the existence of dark matter. *Astrophys. J. Lett.*, 648:109, 2006.
- [3] Scott Dodelson. *Modern Cosmology*. Academic Press, 2003.

- [4] M. Davis, G. Efstathiou, C.S. Frenk, and S.D. White. The evolution of large-scale structure in a universe dominated by cold dark matter. *Astrophys. J.*, 292:371, 1985.
- [5] G. Bertone, D. Hooper, and J. Silk. Particle dark matter: evidence, candidates, and constraints. *Phys.Rept.*, 405:279, 2005.
- [6] W.N. Johnson III, F.R. Harnden Jr., and R.C. Haymes. The spectrum of low-energy gamma radiation from the galactic-center region. *Astrophys. J.*, 172:L1, 1972.
- [7] M. Leventhal, C.J. MacCallum, and P.D. Stang. Detection of 511 keV positron annihilation radiation from the galactic center direction. *Astrophys. J.*, 225:L11, 1978.
- [8] L.X. Cheng and M. Leventhal. A maximum entropy map of the 511 keV positron annihilation line emission distribution near the galactic center. *Astrophys. J. Lett.*, 481:L43, 1997.
- [9] W.R. Purcell and L.X. Cheng. OSSE mapping of galactic 511 keV positron annihilation line emission. *Astrophys. J.*, 491:725, 1997.
- [10] G. Weidenspointner et al. The sky distribution of positronium annihilation continuum emission measured with SPI/INTEGRAL. *Astron. Astrophys.*, 450:1013, 2008.
- [11] G. Weidenspointner et al. The sky distribution of 511 keV positron annihilation line emission as measured with INTEGRAL/SPI. astro-ph/0702621.
- [12] G. Weidenspointner et al. An asymmetric distribution of positrons in the galactic disk revealed by gamma rays. *Nature*, 451:159, 2008.
- [13] P.A. Milne, J.D. Kurfess, R.L. Kinzer, and M.D. Leising. Supernovae and positron annihilation radiation. *New Astron. Rev.*, 46:558, 2002.
- [14] G. Bertone, A. Kusenko, S. Palomares-Ruiz, S. Pascoli, and D. Semikoz. Gamma ray bursts and the origin of galactic positrons. *Phys. Lett.*, B636:20, 2006.
- [15] P.A. Sturrock. A model of pulsars. *Astrophys. J.*, 164:529, 1971.
- [16] R. Ramaty and R.E. Lingenfelter. Gamma-ray evidence for a stellar-mass black hole near the galactic center. *N.Y. Acad. of Sci. Ann.*, 571:433, 1989.
- [17] B. Kozlovsky, R.E. Lingenfelter, and R. Ramaty. An asymmetric distribution of positrons in the galactic disk revealed by gamma rays. *Astrophys. J.*, 316:801, 1987.
- [18] B.W. Lee and S. Weinberg. Cosmological lower bound on heavy-neutrino masses. *Phys. Rev. Lett.*, 39:165, 1977.
- [19] C. Boehm and P. Fayet. Scalar dark matter candidates. *Nucl.Phys.*, B683:219, 2004.

- [20] Y. Ascasibar, P. Jean, C. Boehm, and J. Knodlseder. Constraints on dark matter and the shape of the Milky Way dark halo from the 511 keV line. *Mon. Not. R. Astron. Soc.*, 368:1695, 2006.
- [21] C. Boehm, Y. Farzan, T. Hambye, S. Palomares-Ruiz, and S. Pascoli. Are small neutrino masses unveiling the missing mass problem of the universe? hep-ph/0612228.
- [22] J. Beacom and H. Yuksel. Stringent constraint on galactic positron production. *Phys. Rev. Lett.*, 97:071102, 2006.
- [23] C. Jacoby and S. Nussinov. Some comments on an MeV cold dark matter scenario. *JHEP*, 05:017, 2007.
- [24] Particle Data Group Collaboration (C. Amsler et al.). Review of particle physics. *Phys. Lett.*, B667:1, 2008.
- [25] P. Fayet. U-boson production in  $e^+e^-$  annihilations,  $\psi$  and  $\Upsilon$  decays, and light dark matter. *Phys. Rev.*, D75:115017, 2007.
- [26] C. Boehm and J. Silk. A new test of the light dark matter hypothesis. *Phys. Lett.*, B661:287, 2008.
- [27] Y. Kahn, M. Schmitt, and T. Tait. Enhanced rare pion decays from a model of MeV dark matter. *Phys. Rev.*, D78:115002, 2008.
- [28] S. Drell. Direct decay  $\pi^0 \rightarrow e^+e^-$ . *Nuov. Cim.*, XI:693, 1959.
- [29] E. Abouzaid et al. Measurement of the rare decay  $\pi^0 \rightarrow e^+e^-$ . *Phys. Rev.*, D75:012004, 2007.
- [30] A. Dorokhov and M. Ivanov. Rare decay  $\pi^0 \rightarrow e^+e^-$ : theory confronts KTeV data. *Phys. Rev.*, D75:114007, 2007.
- [31] David Griffiths. *Introduction to Elementary Particles*. Wiley and Sons, 1987.
- [32] Anthony Zee. *Quantum Field Theory in a Nutshell*. Princeton University Press, 2003.
- [33] F.J. Rogers, H.C. Graboske Jr., and D.J. Harwood. Bound eigenstates of the static screened Coulomb potential. *Phys. Rev.*, A1:1577, 1970.
- [34] D. Finkbeiner, T. Slatyer, N. Weiner, and I. Yavin. PAMELA, DAMA, INTEGRAL, and signatures of metastable excited WIMPs. arXiv:0903.1037.
- [35] D. Merritt, J.F. Navarro, A. Ludlow, and A. Jenkins. A universal density profile for dark and luminous matter? *Astrophys. J.*, 624:L85, 2005.
- [36] M. Lattanzi and J. Silk. Can the WIMP annihilation boost factor be boosted by the Sommerfeld enhancement? *Phys. Rev.*, D79:083523, 2009.

- [37] Malcolm Longair. *High Energy Astrophysics, vol. 2*. Cambridge University Press, 1994.
- [38] J. Navarro, C.S. Frenk, and S.D. White. A universal density profile from hierarchical clustering. *Astrophys. J.*, 490:493, 1997.
- [39] C. Boehm, D. Hooper, J. Silk, M. Casse, and J. Paul. MeV dark matter: Has it been detected? *Phys. Rev. Lett.*, 92:101301, 2004.
- [40] O. Adriani et al. Observation of an anomalous positron abundance in the cosmic radiation. *Nature*, 458:607, 2009.
- [41] R. Bernabei et al. First results from DAMA/LIBRA and the combined results with DAMA/NaI. *Eur. Phys. J.*, C56:333, 2008.